metals

MDPI

Article

Study on Solidification Structure Evolution of Direct-Chill Casting High Purity Copper Billet Using Cellular Automaton-Finite Element Method

Yonghui Jia [1,2], Dazhi Zhao [2], Chunyu Li [1,2], Lei Bao [1,*], Qichi Le [1], Hang Wang [1,2] and Xuan Wang [1,2]

[1] Key Lab of Electromagnetic Processing of Materials, Ministry of Education, Northeastern University, Shenyang 110819, China; jyh5499@163.com (Y.J.); lichunyu8217@gmail.com (C.L.); qichil@mail.neu.edu.cn (Q.L.); wanghang7@126.com (H.W.); 18842396165@163.com (X.W.)

[2] School of Materials and Engineering, Northeastern University, Shenyang 110819, China; zhaodz@smm.neu.edu.cn

* Correspondence: baolei@epm.neu.edu.cn; Tel.: +86-24-8368-3312

Received: 26 June 2020; Accepted: 31 July 2020; Published: 5 August 2020

Abstract: A heat transfer model and a cellular Automation-Finite Element (CAFE) coupling model were established to analyze the solid/liquid (S/L) interface and solidification structure evolution of high purity copper Direct-chill (DC) casting billet under different casting conditions. The simulation and actual experimental results of liquid sump shape and solidification structure were first compared to verify the accuracy of the model. It is proved that the model is effective for simulating the solidification structure of the actual DC casting high purity copper billet. After that, the model was used to predict the solidification structure under different casting temperatures, casting speeds, and heat transfer coefficients. It is shown that, with the increase of casting temperature, the grain size decreases first and then increases. There is a compromise between grain size and its uniformity, and the grain size is more uniform at higher casting temperature. With the increase of casting speed, the depth of liquid sump and the height of the S/L interface increase, but the total grain number of the billet cross-section decreases gradually. As the heat transfer coefficient increases, the depth of the casting liquid sump becomes shallow, but the height of the solid-liquid interface increases and the grain size increases gradually. For the preparation of high purity copper billets with large cross-sectional dimensions by DC casting, a fine solidified structure could be obtained by appropriately reducing the casting speed and cooling intensity.

Keywords: temperature field; solidification structure; high purity copper; cellular automaton-finite element; direct-chill casting

1. Introduction

The high purity copper target can meet the nano-level wiring requirements of integrated circuits due to its advantages of low resistivity, good conductivity, high electromigration resistance, and excellent heat dissipation [1,2]. It is one of the most commonly used metal target products in the electronics industry. Simultaneously, the rapid development of the semiconductor sputtering process not only requires the ultra-high purity of copper target but also puts forward more and more strict requirements for the grain size, texture, microstructure uniformity control, high-precision molding processing, etc. [3,4]. Therefore, the preparation of high-purity copper target billet is facing increasing challenges in both microstructure and sectional dimension.

The development of copper sputtering targets mainly focuses on grain size, microstructure orientation control, and its uniformity [5,6]. In particular, the semiconductor industry has quite

stringent requirements on the grain size control and crystal orientation of the target surface, and in general, the grain size of the target must be controlled below 100 μm [7]. Therefore, controlling grain size is significant for the preparation of metal targets. The literature suggests that for sputtering targets of the same composition, the sputtering rate of fine-grained targets is faster than coarse-grained sputtering targets; Uniform grain sizes means a more uniform thickness distribution for the deposited film of targets [8]. The processing technique of the target material mainly includes billet preparation, homogenization treatment, pressure processing, and mechanical processing, etc. [9]. The grain size and structural uniformity of the initial billets are essential for subsequent processing. At present, the preparation methods of high purity billets mainly include the following: temperature controlled mold continuous casting (TCMCC) [10], vacuum continuous casting (VCC) [11,12], and up-drawing continuous casting [13]. TCMCC technique is an effective and new method for preparing metals with precise dimensions, but the size of the billet that can be made is small, and the diameter of the billet in [10] is 20mm. VCC is one of the main methods used to produce higher purity copper rods. However, the entire casting equipment needs to be in a vacuum environment during VCC, thus this method has a significant limitation on the size of the equipment, making it unable to meet the preparation requirement of large size billet. The up-drawing continuous casting method is usually applied in combination with the subsequent deformation processing, which has the advantages of short process, high efficiency and energy saving, and low oxygen content. However, due to the characteristics of the up-drawing casting process, it can currently only meet the preparation of billets with a diameter of 50~150 mm. DC casting techniques is a major technological route in the production of large-size billets for further extrusion deformation. Thus, solidification is a significant part of the DC casting process for high purity oxygen-free copper. It is generally appreciated that the microstructure of the billets determines the properties of the billet. Moreover, because solidification is the process of moving individual atoms from the liquid to a more stable position in the solid alloy lattice, the distances over which atoms must move during solidification are also important [14]. For these reasons, the discussion of the changes in solid/liquid (S/L) interface during DC casting is significant for controlling solidification structures.

Traditional approaches are conducted on the basis of physical observation and metallurgical analysis on actual casting under various operating conditions, which will involve a lot of resources and time. Therefore, it is desirable to utilize numerical modeling techniques to simulate the solidification microstructure. Based on the mathematical models that describe solidification at the macroscale (the solution of conservation equations for mass, energy, and momentum) and describe solidification at the mesoscale (the Cellular Automaton (CA) technique), the evolutions of macro-physical fields and grain morphology can be obtained [14]. Rappaz and Gandin [15] established two-dimensional CA model, with the help of quasi-continuous nucleation model to simulate the heterogeneous nucleation during solidification and based on the KGT model to calculate the growth kinetics of dendrite tip, calculated the grain structure of Al-Si alloy with a different mass fraction under uniform temperature field, investigated the phenomena of columnar to equiaxed crystal transition and competitive growth of the columnar crystal, etc. [16]. Luo et al. [17] established the CA-FD model of solidification microstructure of continuous casting billet according to the interfacial solute conservation growth kinetics, simulated the solidification microstructure of Fe-0.6wt.%C alloy continuous casting process, and investigated the effect of different superheat and secondary cooling specific water quantity on the microstructure of the billet, indicating that increasing the superheat will promote the growth of columnar crystals and reduce the proportion of equiaxed crystals; low superheat casting is necessary for inhibiting the growth of columnar crystals and expanding the equiaxed regions of the center. Tsai et al. [18] utilized a Three-Dimensional Cellular Automaton (3D-CA) model and the finite difference method simulate the macro-temperature field, nucleation, and grain growth of a pure copper rod, and they found that there is a tendency for the grain growth direction to change from axial to radial with increasing casting speed. Hou et al. [19] simulated the solidification structure of the continuous casting billet by using CAFE method and studied the solidification structure and the compactness degree of the central equiaxed grain zone in the billet under different conditions. Li et al. [20] established a transient 2D coupled CAFE

mathematical model to investigate the heat transfer, solidification behavior, and microstructure of the H13 die steel, the evolution of the multiscale phenomena with growing of the ingot was considered by the varying boundary conditions.

The present study aimed to systematically reveal the effect of casting parameters on heat transfer behavior and solidification structure of high purity copper billet. It provided a theoretical basis for improving the quality of billet metallurgy through the adjustment of casting parameters. Based on the industrial DC casting system and production process of high purity copper billets, a comprehensive mathematical model of high purity copper DC casting was established, including the macro heat transfer model and solidification model. The accuracy of the model was validated based on the experimental results. Intrinsic correlation between casting parameters, melt heat transfer behavior, and solidified structure were discussed in detail.

2. Model and Method Descriptions

2.1. Experimental Material and Methods

The experimental material was high purity oxygen-free copper; its purity is 4N, which means that the mass fraction of Cu is over 99.99 wt. %. In this study, the heat enthalpy method is used to deal with the heat conduction problem of phase transition. This method is to establish a unified energy equation in the whole computational region (including liquid phase, solid phase, and solid/liquid interface) by using the enthalpy method to calculate the heat enthalpy distribution and then determine the solid/liquid interface. Therefore, this method does not need to track the interface and separate the solid-liquid phase, which is more suitable for multidimensional cases. Figure 1 shows the variations of thermal conductivity, density, enthalpy, and Newtonian viscosity of the material used in the present study with the temperature during solidification, which were simulated by ESI's ProCAST software.

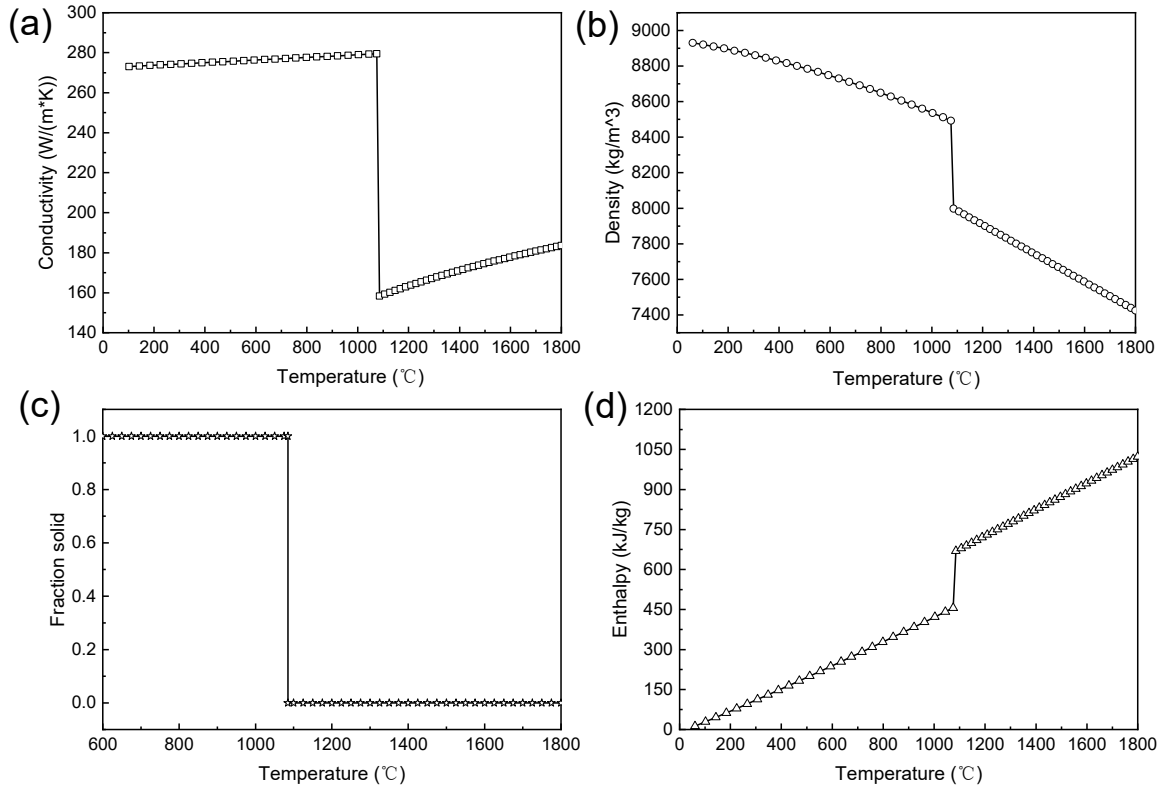

Figure 1. Material properties used in this study, including conductivity (**a**), density (**b**), fraction solid (**c**), and enthalpy (**d**).

Figure 2 shows the experimental setup and the casting process of the billet. The equipment used in the present study is consisted of induction melting furnace, casting crystallizer system, and data recorder. The crystallizer system is comprised of a water-cooled system, inner ring (Φ300mm), also known as inner sleeve, and dummy bar installation. The removal of heat through the mold wall is called primary cooling. The cooling water flows out of the bottom of the mold through a series of holes, resulting in a series of water jets in direct contact with the surface of the billet, constituting secondary cooling.

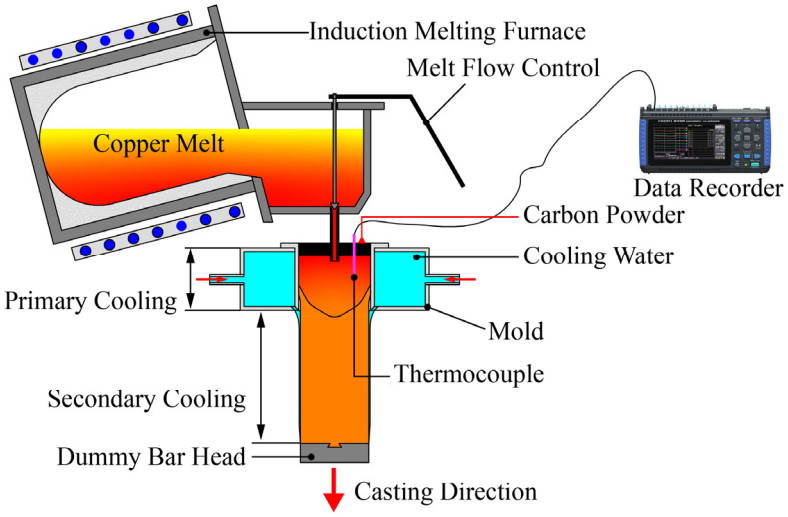

Figure 2. Schematic diagram of the experimental setup.

The copper was melted in an induction melting furnace under the protection of carbon powder to prepare the molten melt. When the copper plate was completely melted, the melt was kept 20–30 min in casting temperature, and then poured into the mold to produce a billet with a diameter of 300 mm until the completion of solidification. In the present experiment, casting speed was 0.00125 m/s; the velocity of the cooling water flow was 15 m^3/h. Finally, the sample was taken from casting billets and polished by a traditional approach for metallographic preparation, and then etched with a solution of 30% nitric acid.

2.2. Heat Transfer Model

2.2.1. Governing Equations

According to the heat transfer characteristic of billet during DC casting, take a micro-element with a length of dx, a width of dy, and a height of dz from the billet, and move down with the billet. The governing equation for the three-dimension heat transfer calculation is written as Equation (1) [16], where heat transfer along the z direction is weak (about 3–6%) and can be ignored. The latent heat during solidification was incorporated into the calculation.

$$\rho C_p \frac{\partial T}{\partial t} = \lambda\left(\frac{\partial^2 T}{\partial^2 x} + \frac{\partial^2 T}{\partial^2 y} + \frac{\partial^2 T}{\partial^2 z}\right) + \rho L \frac{\partial f_s}{\partial t} \quad (1)$$

where ρ is the density, C_p is the specific heat, λ is the thermal conductivity, T is temperature, t is time, and $\rho L \frac{\partial f_a}{\partial t}$ indicates the latent heat generated at the S/L interface during dendrite growth.

2.2.2. Boundary Conditions

Heat transfer and solidification in a stable casting stage were studied. Although the melt flow is a transient process because of the characteristic of the fluid, the casting velocity and heat transfer

process are basically stable during steady-state casting. In the calculation, a three-dimension model was established, and the boundary conditions and the relevant formulas and figures are shown in Figure 3. Besides, solid transport boundary equals casting velocity, and the initial temperature condition is casting temperature (T_{cast}), as shown in Equation (2).

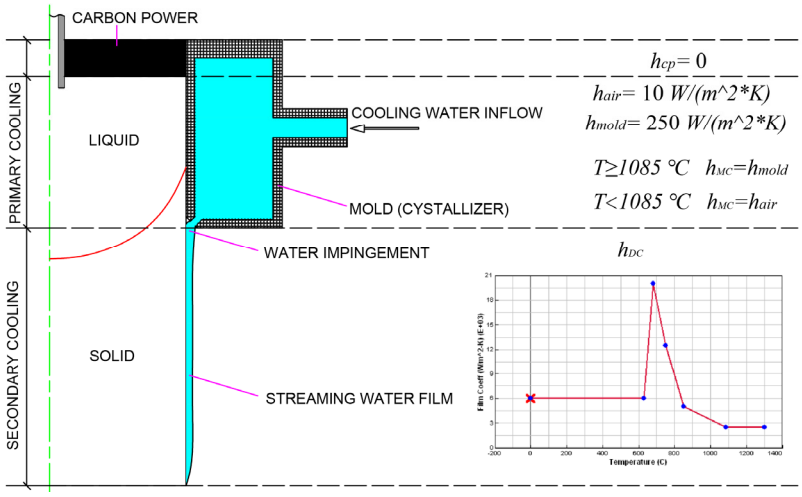

Figure 3. Description of the thermal boundary conditions for the cooling face.

In this study, temperature distribution and solidification structures under different casting parameters were studied systemically. The geometrical properties, operating conditions, and detailed research parameters are listed in Table 1. The Liquidus of high purity copper used in this study is 1085 °C. In the numerical simulation of solidification, the transition temperature of the metal melt from the solid phase to the liquid phase cannot be constant. Therefore, in the calculation process of this study, the liquidus is set to 1085 °C, and the solidus is set to 1084 °C. The choice of casting speed is based on the actual production process of billets and the characteristics of DC casting. The casting speed of 0.00125 m/s is a common speed parameter for producing billets with a diameter of 300 mm, but that does not mean that it is the optimal speed parameter. However, for DC casting, the metal melt flows into the mold first through the primary cooling (weak) of the mold and then through the secondary cooling (strong) directly sprayed by the cooling water. Therefore, it is essential to control the height of the solid-liquid interface. The risk of melt leakage is easy to occur when casting speed is high. When the casting speed is low, the retention time of the melt in the primary cooling zone is longer, which is not conducive to the solidification microstructure refinement, and the production efficiency of low speed casting is too low. Similarly, the choice of temperature is also based on the above reasons. The casting temperature of 1225 °C in Table 1 is a common parameter for producing billets with a diameter of 300 mm. The limited high temperature and low temperature casting is a safe casting strategy, and the limited low temperature casting is beneficial to the microstructure refinement in theory. For the heat transfer coefficient, first, obtain the heat transfer coefficient shown in Figure 3 based on the experimental results, and then estimate the adjustable range of its value based on the actual cooling water quantity, billet size, and the characteristics of DC casting.

$$T(x,\ y,\ z) = T_{cast} \tag{2}$$

Table 1. Geometrical properties and operating conditions used in the calculation.

Parameters	Values
Diameter of the billet (m)	0.300
Height of the billet (m)	0.525
Height of the mold (m)	0.265
Liquidus (°C)	1085
Solidus (°C)	1084
Casting temperature, T_{cast} (°C)	1150
	1175
	1200
	1225
	1250
Casting speed (m/s)	0.00100
	0.00125
	0.00150
The intensity of cooling water (W/(m^2·K))	0.5h (Figure 2)
	h (Figure 2)
	2h (Figure 2)

2.3. CAFE Model

2.3.1. Nucleation Model

Without thermosolutal convection to transport dendrite fragments from the mushy zone to the bulk liquid, it is reasonable to assume that nucleation of equiaxed grains is based on heterogeneous nucleation mechanisms [14]. Based on the heterogeneous nucleation theory, the continuous nucleation model and instantaneous nucleation model have been developed; they are empirical in essence and rely heavily on metal- and process-specific experimental data. In this work, based on the Gaussian distribution, continuous nucleation was employed to describe the heterogeneous nucleation occurring at the mold wall and in the bulk of melt [20]. The continuous nucleation model (Equation (3)) assumes a continuous dependency of n on temperature [15,21]. Some mathematical relationship is then provided to correlate nucleation velocity, dn/(d(Δt)), with undercooling, Δt, cooling rate, or temperature. A summation procedure is carried out to determine the final number of nuclei [14].

$$\frac{dn}{d(\Delta t)} = \frac{n_{max}}{\sqrt{2\pi}\cdot\Delta T_\sigma} \exp\left[-\frac{1}{2}\left(\frac{\Delta T - \Delta T_n}{\Delta T_\sigma}\right)^2\right] \quad (3)$$

where ΔT_n is the average nucleation undercooling, ΔT_σ is the standard deviation of the nucleation undercooling, and n_{max} is the maximum density of grains given by the integral of the total distribution (from zero undercooling to infinite undercooling).

2.3.2. Growth Kinetics Model

Undercooling is necessary to drive the solidification phase transition. General undercooling at the S/L interface can be written as Equation (4).

$$\Delta T = \Delta T_c + \Delta T_t + \Delta T_k + \Delta T_r \quad (4)$$

where ΔT_c, ΔT_t, ΔT_k and ΔT_r are the undercooling contributions associated with temperature difference due to solute diffusion, temperature difference due to heat flow, kinetics, and the undercooling due to curvature, respectively.

The core of dendrite growth kinetics calculation is to determine the velocity of the S/L interface, which mainly depends on the local solute concentration and temperature distribution. In the current work, the growth rate of the dendrite tip was calculated using the KGT model. KGT model is based on Mullins and Sekerka interfacial stability theory, describing the dendrite tip growth process kinetic

model. The KGT model is used to describe columnar (directional) growth of dendrites, including growth rates in the range of the limit of absolute stability [22]. The simulation results of this model can well show the competition of columnar crystals and the growth of central equiaxed crystals. The expression of the growth rate of the dendrite tip is as follows (Equation (5)):

$$V(\Delta T) = a_2 \Delta T^2 + a_3 \Delta T^3 \quad (5)$$

where a_2 and a_3 are the fitting coefficients, which were determined by composition of the material and calculated the ProCAST software. Table 2 shows the parameters for microstructure CAFE model of DC casting process.

Table 2. Parameters for microstructure CAFE model of DC casting process.

Cell Size (μm)	Number of Cells in a Block	Nucleation Parameters					
		Volume Nucleation			Surface Nucleation		
		$\Delta T_{v,max}$ (°C)	$\Delta T_{v,\sigma}$ (°C)	$n_{v,max}$ (m^{-3})	$n_{v,max}$ (m^{-3})	$\Delta T_{s,\sigma}$ (°C)	$n_{s,max}$ (m^{-2})
600	10 × 10 × 10	1	0.1	2×10^6	0.1	0.1	5×10^4

2.3.3. Calculation Procedures

The flowchart of the simulation process is shown in Figure 4a. The three-dimensional geometrical model was first established by using 3D modeling software, including billet and crystallizer (mold), and then the geometry model was imported into ESI's calculation software (updated ProCAST). By careful consideration of calculation precision and calculation time, the computation domain was divided into 48,218 2D elements and 760,283 3D elements, as shown in Figure 4b. According to the actual production process conditions, the boundary conditions of the temperature field and microstructure calculation were applied. Then, the temperature field was calculated, finally, the solidification structure was simulated by the CAFE simulation. CAFE simulation is a macro-micro cellular automaton model, established by the coupling cellular automaton model (CA) with the finite element method (FE). The FE mesh is used to calculate the heat transfer process, and the CA cell (much smaller grid) is used to calculate the grain growth process. In the solidification region, temperature field is first calculates with a coarse grid (i.e., FE). Within this grid, it is divided into finer and more uniform nodes, in which CA model is used for nucleation and growth calculation. CA nodes are automatically generated [23].

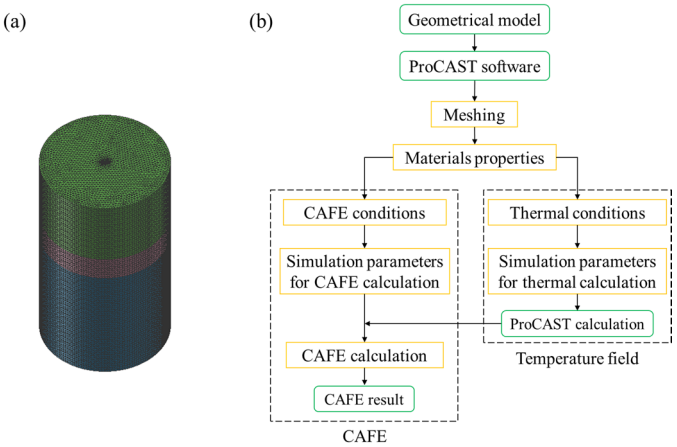

Figure 4. Meshes of heat transfer model of DC casting for high purity copper billet (**a**); and calculation flowchart used in the current work (**b**).

3. Model Validation

3.1. Mesh Size

In this work, the effects of three different sizes of meshes (4, 6, and 8 mm) on the simulation results were studied. The results are shown in Figure 5. It can be seen that the calculation can converge under three mesh sizes. However, the temperature at point C rises slightly (~1 °C) as the mesh size decreases when the casting reaches stable stage. From the calculation results of the current temperature difference of 25 °C, the temperature difference of 1 °C is not enough to have a significant impact on the calculation results, taking into account the calculation time and calculation accuracy, mesh size of the model in this study is 6 mm.

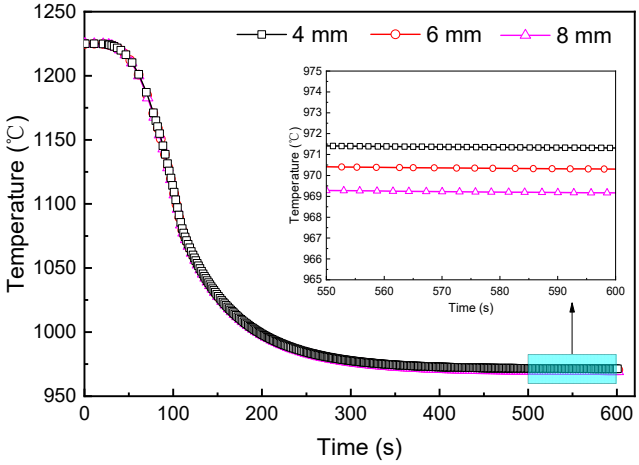

Figure 5. Temperature change at point C with time under different mesh sizes.

3.2. Comparison of Simulation and Experimental Results

The accuracies of the heat transfer model and the CAFE model were verified according to the actual production process, casting parameters, and experimental results. The validation of the heat transfer model was performed by a comparison of the simulated liquid sump shape (solidus) and the actual measurement result, as shown in Figure 6. Figure 6a shows the temperature variation in the process of reaching a stable state along the centerline of billet. Figure 6b shows the simulated and experimental measurement liquid sump shape where the red region is a liquid phase and the gray area is a solid phase. The results indicate that the liquid sump during casting can be well predicted by this model. The effectiveness of the CAFE model was validated by comparing the simulated solidification structure with the experimental solidified structure.

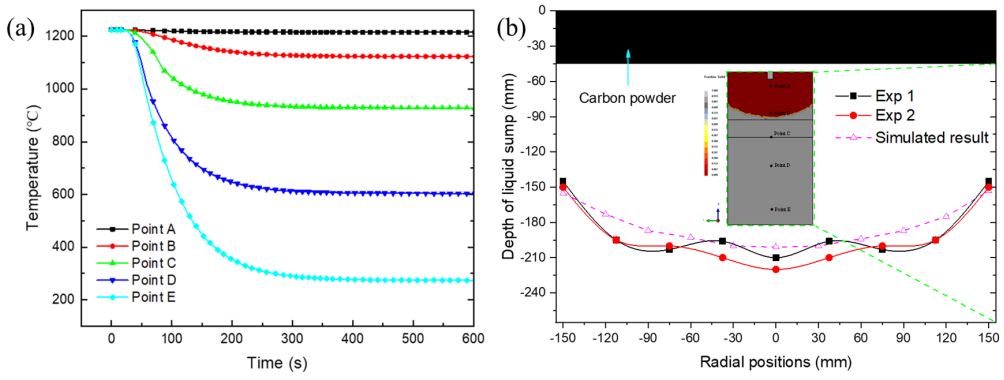

Figure 6. The temperature variation in the process of reaching a stable state along the centerline of billet (**a**), simulated and experimental measurement liquid sump shape (**b**).

Figure 7a shows the simulated solidification structures along the cross-section and longitudinal section of billet. Figure 7b is the experimental results. It shows a good agreement between the simulated and experimental results. Consequently, the established model is effective for simulating the solidification structure of the actual DC casting high purity copper billet.

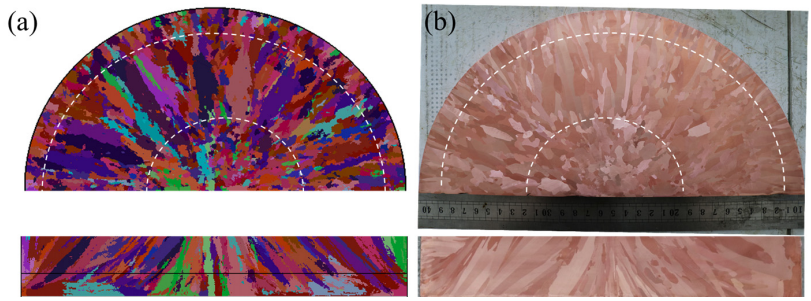

Figure 7. Cross-sectional and longitudinal section solidification structures of the simulated result (**a**) and actual casting billet (**b**).

4. Results and Discussion

4.1. The Effect of Casting Temperature on Solidification Structure Evolution

Figure 8 shows the simulated results of the solidification structure under different temperatures. Figure 8a–e shows the cross-section structure of billet, while Figure 8a-1–e-1 presents the longitudinal section structure of billet. The casting speed and cooling intensity are the same, i.e., 0.00125 m/s and 15 m^3/h, respectively.

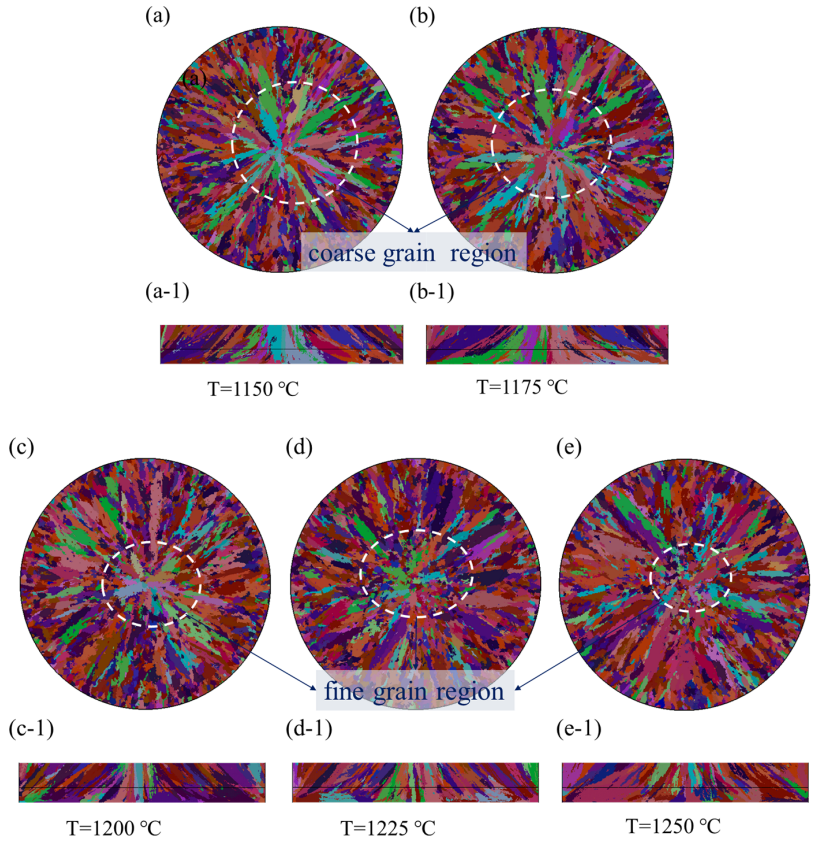

Figure 8. Simulated solidification structure under different casting temperature. (**a**–**e**) cross section of billet; and (**a-1**–**e-1**) longitudinal section of billet.

As shown in the figure, the solidification structure of the billet cross-section is composed of the edge fine crystal region, columnar structure region, and central fine crystal region. As the casting temperature increases, the area of columnar structures in the center of billet decreases, and that of fine crystals region is enlarged. The width of the fine grain area at the edge of the billet gradually decreases, which means that the columnar structure gradually moves from the center of the billet to the edge. The reason for this is that the temperature gradient along the cross-section of billet decreases. A thin shell was formed at the edge of the mold during low-temperature casting (1150–1200 °C), as shown in Figure 9. Because of the solidification shrinkage of copper, the air gap formed between the solidified region and the wall of the mold, and the heat dissipation of melt in the liquid sump decreased sharply. Moreover, it is difficult for pure metals to produce crystal-free at the mold wall. The solidification front is flat growth, so its preferential growth is not apparent. The solidification front grows in a plane; thus, its preferential growth is not obvious. The solidification front adopts a planar growth mode to extend inward against the direction of heat flow and become a columnar crystal structure [24,25]. At higher casting temperatures, the shell at the mold wall is no longer formed, and the depth of liquid sump decreased, as shown in Figure 9d,e. Under the circumstances, heat extraction along the cross-section of the billet is faster, and the temperature distribution is more uniform. During solidification, the angle between dendrite growth direction and casting direction decreases, thus the solidification structure of the billet cross-section presents smaller grain size, and the width of fine grain area in the edge of ingot becomes narrower.

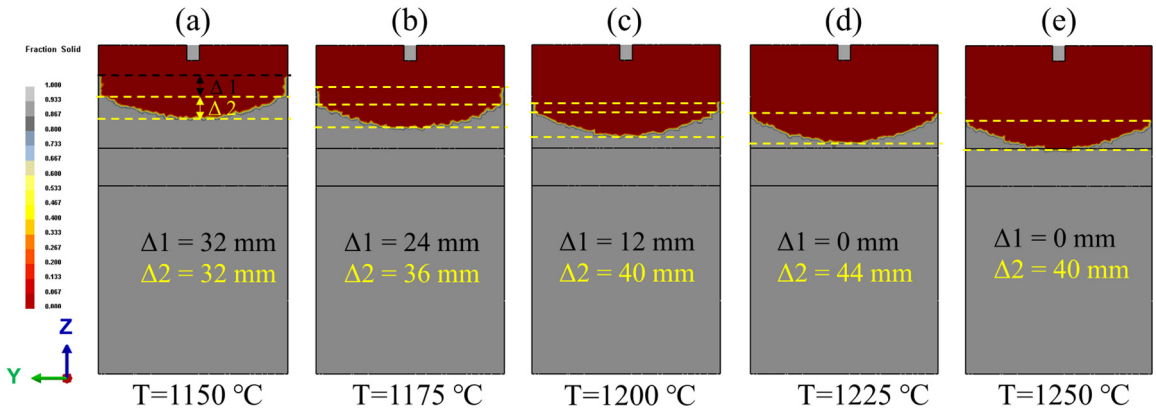

Figure 9. Liquid sump shape and depth under different casting temperature conditions. The casting speed and cooling intensity are the same, i.e., 0.00125 m/s and 15 m^3/h, respectively; casting temperature conditions are 1150 °C (**a**), 1175 °C (**b**), 1150 °C (**c**) 1200 °C, 1225 °C (**d**), and 1250 °C (**e**), respectively.

The total grain number and the grain size distribution of the whole cross-section of the billet under each casting temperature condition were counted, as shown in Figure 10. The results show that, with the increase of casting temperature, there is a maximum grain quantity (at 1200 °C), which is closely related to the heat dissipation and the shape of the liquid sump during solidification. When a solidified shell forms at the edge of the billet earlier, conditions favorable for unidirectional heat dissipation forms near the mold wall. The original isotropic growth conditions are destroyed, which promotes the crystal to grow into columnar along the opposite direction of heat flux and extend to the center of the billet. Statistical results of grain size distribution shown in Figure 10b indicate that, when casting temperature is lower (1150 and 1175 °C), the grain size of billet cross-section is relatively small, but the proportion of small-sized grains is low. During high-temperature casting (≥1200 °C), the grain size of the billet cross-section is slightly increased, but its percentage is higher than the result of low-temperature casting. It is proved that, at higher casting temperature, the grain size is more uniform. However, with the increase of casting temperature, there is a compromise between grain size and its uniformity. When the casting temperature is lower, the grain size at the edge of the billet is smaller, and the grain size at the center is larger. At higher casting temperatures, the grain size in the center of the

billet gradually decreases, but the fine-grained regions at the edges decrease. Thus, at higher casting temperatures, the grain size is relatively uniform, but the grain size is larger. A similar phenomenon was observed in the studies of Tsai et al. [18].

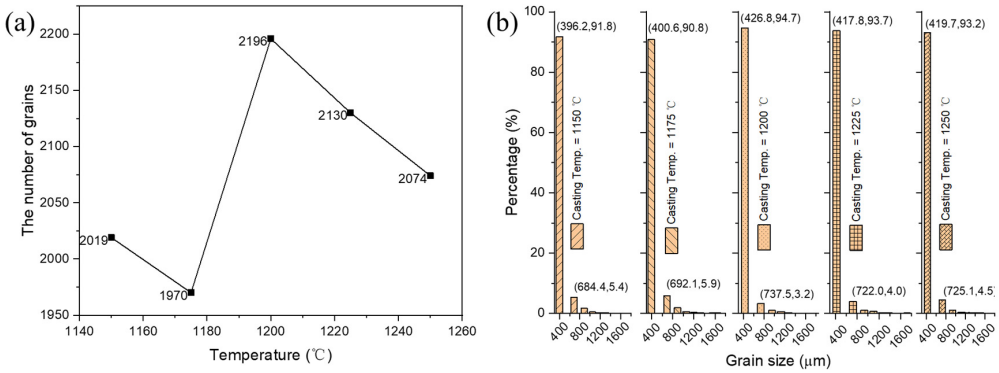

Figure 10. The number of grains and grain size distribution on the cross-section of billet with different casting temperatures, where (**a**) is the variations of total grains numbers, and (**b**) is the percentage of grains of different sizes.

4.2. The Effect of Casting Speed on Solidification Structure Evolution

The influence of casting speed (0.00100, 0.00125, and 0.00150 m/s) on solidification structure was studied under the same casting temperature (1225 °C) and cooling strength (*h*, as shown in Figure 3). Figure 11 shows the simulated results of the solidification structure under different casting speed. Figure 11a–c is the cross-section structure of billet, while Figure 11a-1–c-1 presents the longitudinal section structure of billet. Similarly, the cross-sectional structure of the billet is composed of the edge fine crystal area, the center fine crystal area, and the columnar crystal structure between them. As shown in Figure 11, with the increase of casting speed, the fine crystal area in the center of the billet gradually disappears and changes into a columnar crystal structure that gradually penetrates into the center of the billet. The reason for this is that, as the casting speed decreases, the residence time of the metal melt in the crystallization zone is prolonged so that the time required to transfer the superheat of the melt is relatively reduced, which promotes the growth of the center fine crystals and inhibits the development of columnar crystals. The temperature variation of the melt during solidification is shown in Figure 12. Moreover, with the increase of casting speed, the depth of liquid sump increases obviously, and the position of S/L interface in the mold shifts down significantly, as shown in Figure 13, which means that the temperature gradient of radial heat transfer increases and the angle between the crystal growth direction and the casting direction increases, thus promoting the full growth of columnar crystals toward the center of the billet.

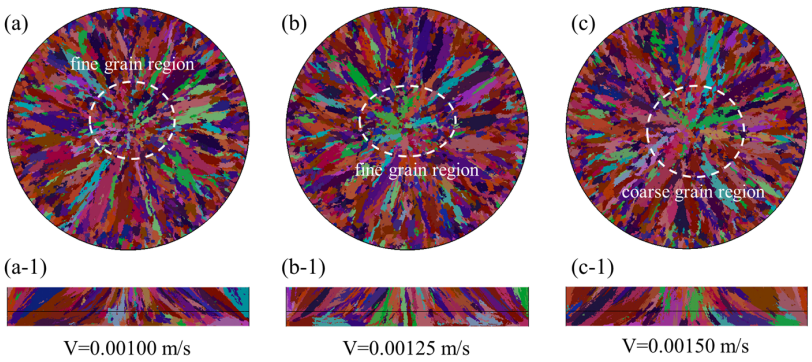

Figure 11. Simulated solidification structure under different casting speed, where (**a**–**c**) are the cross-section structure of billet, (**a-1**–**c-1**) present the longitudinal section structure of billet; the cast speed conditions are 0.00100 m/s (**a**,**a-1**), 0.00125 m/s (**b**,**b-1**), and 0.00125 m/s (**c**,**c-1**), respectively.

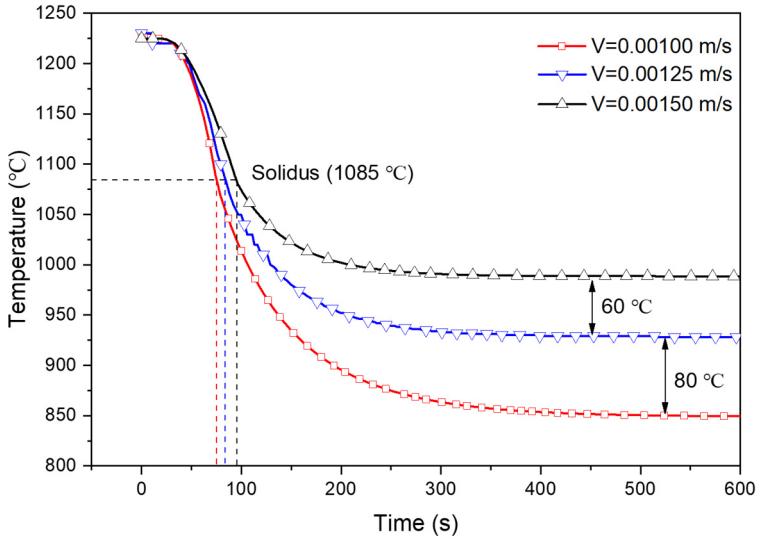

Figure 12. Changes in melt temperature at point C shown in Figure 6 from the initial conditions to steady-state casting at different casting speeds.

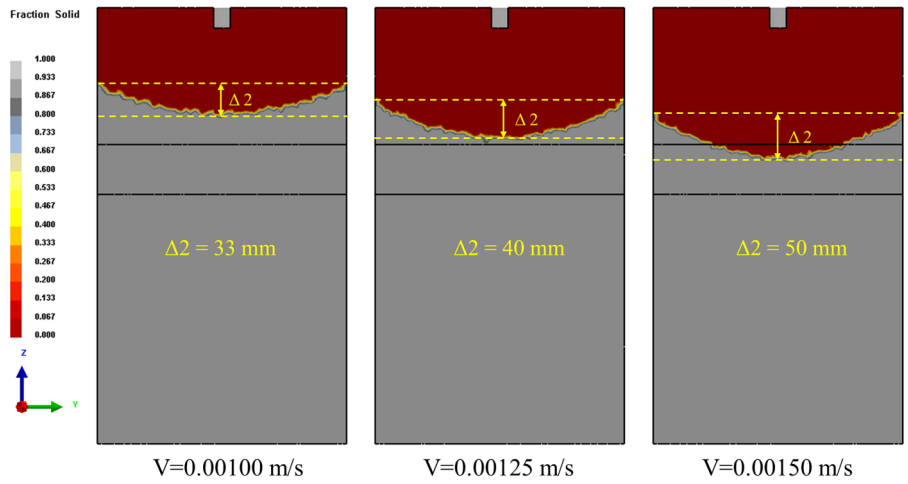

Figure 13. The shape and depth of Liquid sump with different casting speeds.

The statistical result of the total grain number of the whole cross-section under each casting speed indicates that the total grain number decreases with the increase of casting speed, as shown in Figure 14a, which is consistent with the above simulation results. The same trend was also found in [19]. Figure 14b shows the grain size distribution on the cross-section of billet with different casting speeds. It can be seen in the figure that, as the casting speed increases, the grain size gradually decreases. At casting speeds of 0.00100, 0.00125, and 0.00150 m/s, the grain size and proportion of the corresponding section are 451.1 (94.6%), 417.8 (93.7%), and 429.0 μm (94.0%), respectively. It shows that the structural uniformity of billet is better at low casting speed. Therefore, for the DC casting process of high-purity copper, the lower casting speed is conducive to the refinement of the structure. However, the determination of the casting speed in the actual casting process is also closely related to the casting temperature and cooling strength, and the production efficiency should be taken into account at the same time.

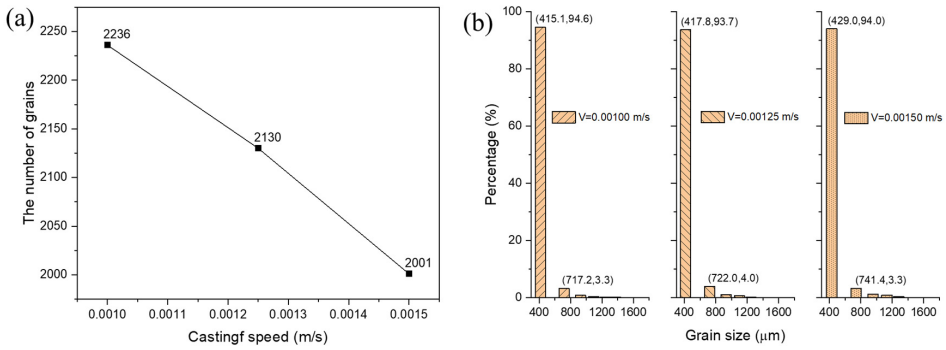

Figure 14. The number of grains and the grain size distribution on the cross-section of the billet with different casting speeds, where (**a**) is the variations of total grains numbers, and (**b**) is the percentage of grains of different sizes.

4.3. The Effect of Heat Transfer Coefficient on Solidification Structure Evolution

The transformation from liquid to solid depends on the extraction of heat from the liquid phase. It is well known that increasing the cooling rate during solidification causes a microstructure with fine grains [26]. Increasing heat flow from the molten metal causes a delay in the nucleation process, so the nucleation starts at a lower temperature with a higher amount of undercooling. However, it is usually very hard or impossible to increase the cooling rate for castings with bigger volumes and thick cross-sections [27]. In the present work, the solidification structure of the billet with different heat transfer coefficient is shown in Figure 15. It can be found that the solidification is still composed of fine and columnar crystal regions. As the heat transfer coefficient increases, the grain size increases gradually. This phenomenon is contrary to the theory in [26]. This is because the depth of liquid sump decreases and the height of the S/L interface ($\Delta 1 + \Delta 2$, as shown in Figure 16) increases with the increase of the heat transfer coefficient. Due to the bigger sectional dimension, heat extraction in the center region of the melt is slower, and increasing the edge cooling would further enhance the radial temperature gradient of the billet. Especially when the heat transfer coefficient is $2h$, the shell with a certain height and thickness appears in the edge region, and the sectional structure is obviously coarsened. This phenomenon has also been discovered during low-temperature casting, and the reason has been explained in the influence of casting temperature on the solidified structure. Research suggests that, when the cooling rate is high, the solidification starts at lower temperatures, and the diffusivity of the solute atoms in solid is low. This situation results in a delay in the formation of the undercooling zone, which allows more time for the existing grains to grow larger. It can be concluded that there is a critical value of cooling rate for every alloy that higher cooling rates than this value cause grain coarsening instead of grain refinement [28]. Increasing cooling rate during solidification is hard or impossible for the high purity copper billet with a bigger sectional dimension.

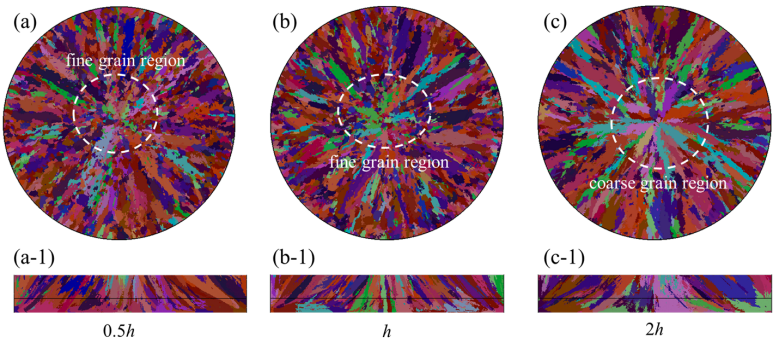

Figure 15. Simulated solidification structure under different heat transfer coefficient, where (**a**–**c**) are the cross-section structure of billet, (**a-1**–**c-1**) present the longitudinal section structure of billet; the heat transfer conditions are $0.5h$ (**a**,**a-1**), h (**b**,**b-1**), and $2h$ (**c**,**c-1**), respectively.

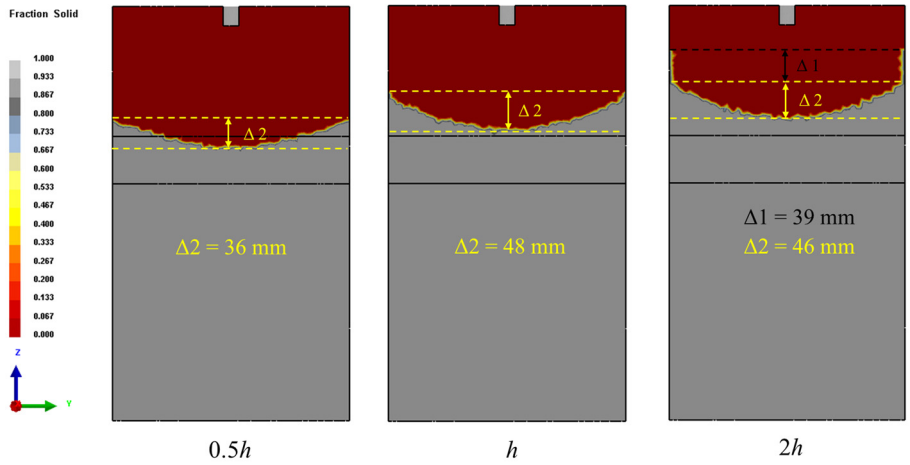

Figure 16. The shape and the depth of liquid sump with different heat transfer coefficient.

Figure 17 shows the total grain number and the grain size distribution of the whole cross-section of the billet with different heat transfer coefficients. Based on the experimental heat transfer conditions, when the heat transfer coefficient is reduced by half (0.5*h*), the number of grains increases slightly. However, when the heat transfer coefficient is doubled, the total number of grains decreases significantly, as shown in Figure 17a. Simultaneously, the statistical result of grain size distribution shown in Figure 17b indicates that, when the heat transfer coefficient is small, the proportion of fine grains in the billet section is more extensive, which suggests that the structure density is higher.

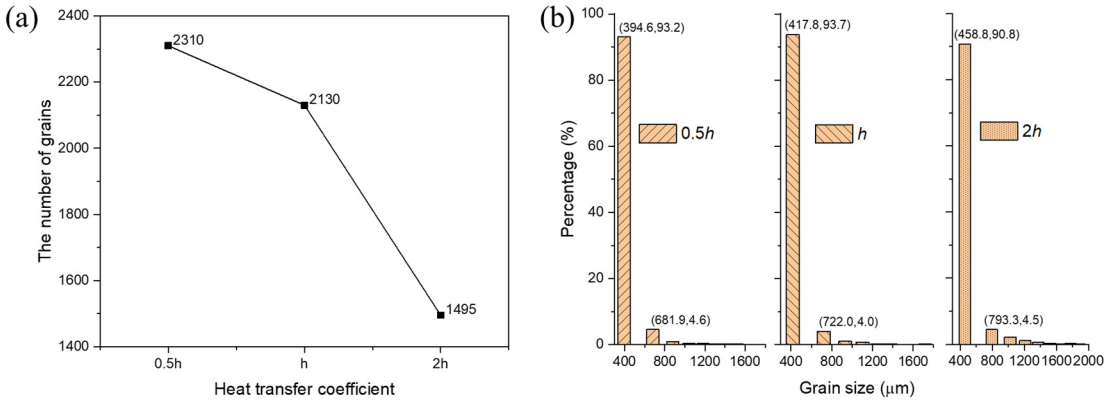

Figure 17. The total grain number and the grain size distribution of the whole cross-section of the billet with different heat transfer coefficients, where (**a**) is the variations of total grains numbers, and (**b**) is the percentage of grains of different sizes.

5. Conclusions

In this study, a heat transfer model and a CAFE coupling model were developed to analyze the evolution of the S/L interface and solidification structure of DC casting high purity copper billets under different casting conditions. The model validation was first achieved by the comparison of the experimental results and simulated results, including the depth of liquid sump and solidification structure. Based on this, the solidification structure evolutions of the billet cross-section were studied under different casting temperature, casting speed, and heat transfer coefficient. The following conclusions can be obtained:

(1) With the increase of casting temperature, the depth of liquid sump increases gradually, but the height of the S/L interface decreases. The grain size decreases first and then increases. There is a compromise between grain size and its uniformity; the grain size is more uniform at higher casting temperature.

(2) With the casting speed increasing, the depth of liquid sump and the height of the S/L interface increase, but the total grain number of the billet cross-section decreases gradually. The structural uniformity of billet is better at lower casting speed.

(3) As the heat transfer coefficient increases, the depth of the casting liquid sump becomes shallow, but the height of the solid–liquid interface increases and the grain size increases gradually.

(4) For the preparation of high purity copper billets with large cross-sectional dimensions by DC casting, a fine solidified structure can be obtained by appropriately reducing the casting speed and cooling intensity.

Author Contributions: Author Contributions: Data curation, Y.J.; Funding acquisition, L.B.; Investigation, Y.J., D.Z., C.L., H.W., and X.W.; Methodology, D.Z.; Project administration, L.B. and Q.L.; Validation, Y.J., D.Z., C.L. and H.W.; Writing—original draft, Y.J.; Writing—review & editing, Y.J. and Q.L. All authors have read and agreed to the published version of the manuscript.

Funding: This research was funded by the National Key Research and Development Program of China, grant number 2017YFB0305504, and the Fundamental Research Funds for the Central Universities, grant number N2009003.

Acknowledgments: The authors of this present research work acknowledge the software support given by the Institute of Metal Research (IMR), Chinese Academy of Sciences (CAS), and give the thanks to L.G. Zheng and J.Y. Sun for their help and advice.

Conflicts of Interest: The authors declare no conflict of interest.

References

1. Hu, C.-K.; Harper, J.M.E. Copper interconnections and reliability. *Mater. Chem. Phys.* **1998**, *52*, 5–16. [CrossRef]
2. Han, S.Z.; Lee, J.; Lim, S.H.; Ahn, J.H.; Kim, K.; Kim, S. Optimization of conductivity and strength in Cu-Ni-Si alloys by suppressing discontinuous precipitation. *Met. Mater. Int.* **2016**, *22*, 1049–1054. [CrossRef]
3. Fu, H.; Xu, S.; Li, W.; Xie, J.; Zhao, H.; Pan, Z. Effect of rolling and aging processes on microstructure and properties of Cu-Cr-Zr alloy. *Mater. Sci. Eng. A* **2017**, *700*, 107–115. [CrossRef]
4. Lei, Q.; Li, Z.; Gao, Y.; Peng, X.; Derby, B. Microstructure and mechanical properties of a high strength Cu-Ni-Si alloy treated by combined aging processes. *J. Alloys Compd.* **2017**, *695*, 2413–2423. [CrossRef]
5. Li, C.; Le, Q.; Hu, K.; Bao, L.; Ma, B.; Jia, Y.; Wang, X.; Zhou, W.; Xu, G. Study on texture and dynamic recrystallization behavior of high purity copper during reverse extrusion. *Mater. Res. Express* **2020**, *6*, 1265e4. [CrossRef]
6. Yu, H.; Wang, L.; Chai, L.; Li, J.; Lu, C.; Godbole, A.; Wang, H.; Kong, C. High thermal stability and excellent mechanical properties of ultrafine-grained high-purity copper sheets subjected to asymmetric cryorolling. *Mater. Charact.* **2019**, *153*, 34–45. [CrossRef]
7. Yu, Z. Development and Current Tendency of High Purity Copper Sputtering Targets. *Shanxi Metall.* **2007**, *5*, 4–6.
8. Shang, Z.; Jiang, X.; LI, Y.; Yang, Y. Sputtering targets used in integrated circuit. *Chin. J. Rare Met.* **2005**, *29*, 475–477.
9. Lo, C.F.; Draper, D. Method for Fabricating Randomly Oriented Aluminum Alloy Sputting Targets with Fine Grains and Fine Precipitates. U.S. Patent No 5,993,575, 30 November 1999.
10. Liu, X.; Liao, W.; Yang, Y. Thermal characteristics and uniformity of microstructures during temperature controlled mold continuous casting profiled copper alloy strip. *Int. Commun. Heat Mass Transf.* **2020**, *110*, 104414. [CrossRef]
11. Tsai, D.C.; Hwang, W.S. Numerical simulation of the solidification processes of copper during vacuum continuous casting. *J. Cryst. Growth* **2012**, *343*, 45–54. [CrossRef]
12. Fu, Y.; Jie, C.; Ning, L.; Luo, D.; Yin, G. Preparation of large sized billets of 99.999% ultrahigh-purity copper by directional solidification directing vacuum melting. *Rare Met. Mater. Eng.* **2011**, *40*, 103–106.
13. Xu, G.; Chen, G.; Yao, Y.; Luo, Y. The new technology of continuous extrusion oxygen-free copper bar. *Spec. Cast. Nonferrous Alloys.* **2014**, *34*, 559–560.
14. Stefanescu, D.M. *Science and Engineering of Casting Solidification*, 2nd ed.; Springer: Berlin, Germany, 2009.

15. Rappaz, M.; Gandin, C.-A. Probabilistic modelling of microstructure formation in solidification processes. *Acta Metall. Et Mater.* **1993**, *41*, 345–360. [CrossRef]
16. Wang, T.; Wei, J.; Wang, X.; Yao, M. Progress and application of microstructure simulation of alloy solidification. *Acta Metallurgica Sinica* **2017**, *54*, 193–203.
17. Luo, S.; Zhu, M.; Louhenkilpi, S. Numerical Simulation of Solidification Structure of High Carbon Steel in Continuous Casting Using Cellular Automaton Method. *ISIJ Int.* **2012**, *52*, 823–830. [CrossRef]
18. Tsai, D.-C.; Hsu, M.-S.; Hwang, W.-S.; Jiang, C.-S. Mathematical Modeling of Solidification Microstructure of Pure Copper by Vacuum Continuous Casting and Its Experimental Verification. *ISIJ Int.* **2010**, *50*, 1843–1850. [CrossRef]
19. Hou, Z.; Jiang, F.; Cheng, G. Solidification Structure and Compactness Degree of Central Equiaxed Grain Zone in Continuous Casting Billet Using Cellular Automaton-Finite Element Method. *ISIJ Int.* **2012**, *52*, 1301–1309. [CrossRef]
20. Li, B.; Wang, Q.; Wang, F.; Chen, M. A Coupled Cellular Automaton–Finite-Element Mathematical Model for the Multiscale Phenomena of Electroslag Remelting H13 Die Steel Ingot. *JOM* **2014**, *66*, 1153–1165. [CrossRef]
21. Skrzypczak, T. Sharp Interface Numerical Modeling of Solidification Process of Pure Metal. *Arch. Metall. Mater.* **2012**, *57*, 1189–1199. [CrossRef]
22. Kurz, W.; Giovanola, B.; Trivedi, R. Theory of microstructural development during rapid solidification. *Acta Met.* **1986**, *34*, 823–830. [CrossRef]
23. Gandin, C.-A.; Rappaz, M. Coupled finite element-cellular automation model for the prediction of dendritic grain structures in solification processes. *Acta Metall. Et Mater.* **1994**, *42*, 2233–2246. [CrossRef]
24. Beddoes, J.; Bibby, M.J. Solidification and casting processes. In *Principles of Metal Manufacturing Processes*; Butterworth-Heinemann: Oxford, UK, 1999; pp. 18–66, ISBN 978-0-340-73162-8.
25. Kurz, W.; Fisher, D.J. *Foundamentals of Solidification*, 2nd ed.; Trans Tech Publications: Stafa-Zurich, Switzerland, 1989.
26. Pryds, N.H.; Huang, X. The effect of cooling rate on the microstructures formed during solidification of ferritic steel. *Met. Mat Trans A* **2000**, *31*, 3155–3166. [CrossRef]
27. Karakulak, E. A review: Past, present and future of grain refining of magnesium castings. *J. Magnes. Alloy.* **2019**, *7*, 355–369. [CrossRef]
28. Ali, Y.; You, G.; Pan, F.; Zhang, M.-X. Grain Coarsening of Cast Magnesium Alloys at High Cooling Rate: A New Observation. *Met. Mat Trans A* **2017**, *48*, 474–481. [CrossRef]